MIT Open Access Articles

Theory of Active Chromatin Remodeling

MIT Massachusetts Institute of Technology

DSpace@MIT

Theory of Active Chromatin Remodeling

Zhongling Jiang and Bin Zhang ⓘ[*]

Department of Chemistry, Massachusetts Institute of Technology, Cambridge, Massachusetts 02139, USA

Nucleosome positioning controls the accessible regions of chromatin and plays essential roles in DNA-templated processes. ATP driven remodeling enzymes are known to be crucial for its establishment *in vivo*, but their nonequilibrium nature has hindered the development of a unified theoretical framework for nucleosome positioning. Using a perturbation theory, we show that the effect of these enzymes can be well approximated by effective equilibrium models with rescaled temperatures and interactions. Numerical simulations support the accuracy of the theory in predicting both kinetic and steady-state quantities, including the effective temperature and the radial distribution function, in biologically relevant regimes. The energy landscape view emerging from our study provides an intuitive understanding for the impact of remodeling enzymes in either reinforcing or overwriting intrinsic signals for nucleosome positioning, and may help improve the accuracy of computational models for its prediction *in silico*.

The eukaryotic genome is packaged into nucleosomes that wrap approximately 147-base-pair (bp) stretch of DNA around histone proteins [1]. Remarkably, nucleosomes do not uniformly cover the whole genome but favor specific locations [2]. The precise position of nucleosomes along the DNA sequence is of critical importance for gene regulation as it determines which part of the genome is accessible [3,4]. In particular, DNA segments occupied by histone proteins will occlude binding by regulatory factors and transcriptional machinery [3,5–10]. In addition, nucleosome positioning may impact the stability of various nucleosome folding motifs [11–14] and correspondingly the compactness of higher order chromatin organization [15,16]. Underpinning the molecular determinants of nucleosome positioning is, therefore, of fundamental interest and can provide insights into genome function.

Both DNA sequence and chromatin remodeling enzymes are crucial for establishing nucleosome positioning *in vivo* [17–21]. Significant progress has been made in understanding the impact of DNA sequence on nucleosome stability [9,22], leading to the discovery of periodic dinucleotides along the nucleosome length [23–25] and intrinsically stiff poly(dA:dT) tracts at nucleosome-depleted regions [26]. On the contrary, a complete understanding for the role of remodeling enzymes has yet to be established [27,28] and conflicting views exist on whether they overwrite or reinforce positioning signals from the DNA sequence [29–32]. The challenge for theoretical studies of remodeling enzymes lies in the fact that they consume ATP to break the detailed balance and drive the system out of equilibrium [33]. Therefore, the thermodynamic analysis that finds great success for studying DNA sequence effect cannot be generalized straightforwardly [34,35]. Though kinetic simulations have helped interpret

experimental observations [30,36,37], a lack of analytical tools like those available for equilibrium systems has significantly hindered the building of intuition for remodeling enzymes. Here, we develop an analytical theory to provide a unified framework for studying the effect of remodeling enzymes, and to reconcile their combined role with intrinsic thermodynamic signals in positioning nucleosomes. In the following, we first introduce a kinetic model for nucleosome positioning that explicitly considers the effect of two different remodeling enzymes. We then show that the kinetic and steady-state properties of this nonequilibrium system can be rigorously mapped onto an effective equilibrium model. Finally, results from numerical simulations are provided to validate the accuracy of the theory.

We used a one-dimensional lattice model to study nucleosome positioning, with each discrete site corresponding to one base pair of DNA (see Fig. 1). The position of a nucleosome i is denoted by its dyad location as x_i. A soft-core potential $v(\Delta x)$ was applied between neighboring nucleosomes separated by Δx base pairs [38,39]. It incurs a finite energetic cost for overlapping nucleosome configurations to account for both the excluded volume effect and transient DNA unwrapping. To focus on the role of remodeling enzymes, we did not explicitly model the DNA sequence effect, and we assume that all lattice sites share the same binding affinity.

For simplicity, we considered systems with fixed nucleosome density and did not include nucleosome formation and disassembly processes. The kinetics of our model consists of only diffusion and active remodeling (see Fig. 1). The diffusion rate was defined as $d = [D/(\Delta x)^2]e^{-\beta \Delta U/2}$, with D being the diffusion coefficient and Δx and ΔU as changes in the nucleosome position
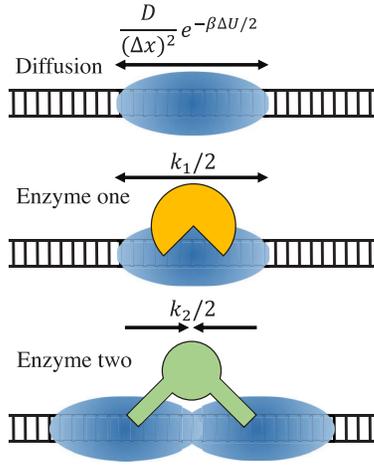
FIG. 1. Illustration of the kinetic model for nucleosome positioning that includes diffusion (top), ATP-driven single-nucleosome remodeling (middle), and ATP-driven remodeling for a pair of nucleosomes (bottom). The DNA is drawn as a black ladder, with nucleosomes shown in blue oval and the two enzymes drawn in yellow and green, respectively. The rates for an elementary step of different dynamics are shown above the arrows.

and interaction energy. Numerous enzymes have been discovered to organize nucleosomes along the DNA by consuming ATP, and we focus on two representative ones with distinct kinetics. Type one enzymes interact with a single nucleosome, and can move it to the left or right by l base pairs with a rate of k_1. These enzymes resemble the function of SWI/SNF [40] and can significantly fluidize nucleosomes to achieve high packing density [30]. Type two enzymes, on the other hand, interact with a pair of neighboring nucleosomes. It can bring them closer to each other and randomly move one of the nucleosomes by l base pairs at a rate of k_2 if the two are within $\Delta x_{max} = 332$ bp [38]. A typical example for these enzymes is the ATP-utilizing chromatin assembly and remodeling factor (ACF) from the ISWI family, which is crucial for the regular spacing of nucleosomes near transcription start sites [41]. Since enzyme rates $k_{1/2}$ are independent of the system's energy, detailed balance is violated.

Our goal is to approximate both kinetic and steady-state properties of the above nonequilibrium system with effective equilibrium models. To make progress, we first describe the dynamical evolution of nucleosome positions $\mathbf{x} = \{x_1, x_2, \ldots, x_n\}$ with the following master equation

$$\frac{\partial}{\partial t}\Psi(\mathbf{x}, t) = (\hat{L}_{FP} + \hat{L}_{NE})\Psi(\mathbf{x}, t), \quad (1)$$

where $\Psi(\mathbf{x}, t)$ is the time dependent probability distribution function and $\hat{L}_{FP} = D\sum_i\{\nabla_i \cdot \nabla_i - \beta\nabla_i[-\nabla_i U(\mathbf{x})]\}$ is the many-body Fokker-Planck operator describing the diffusive dynamics of nucleosomes. $\hat{L}_{NE}$ is the nonequilibrium operator for remodeling enzymes. For type one enzymes, it adopts the following expression

$$\hat{L}_{NE}\Psi(\mathbf{x}, t) = \frac{k_1}{2}\sum_i[\Psi(\mathbf{x}^i_l, t) + \Psi(\mathbf{x}^i_{-l}, t) - 2\Psi(\mathbf{x}, t)], \quad (2)$$

where $\mathbf{x}^i_{\pm l} = \{\ldots, x_i \pm l, \ldots\}$. Similarly, the nonequilibrium operator for type two enzymes can be written as

$$\hat{L}_{NE}\Psi(\mathbf{x}, t) = \frac{k_2}{2}\sum_i[C_{i,i+1}\Psi(\mathbf{x}^i_{-l}, t) + C_{i,i-1}\Psi(\mathbf{x}^i_l, t)$$
$$- (C_{i,i+1} + C_{i,i-1})\Psi(\mathbf{x}, t)], \quad (3)$$

where $C_{i,i\pm 1} = 1$ for $0 < |x_i - x_{i\pm 1}| \leq \Delta x_{max}$ and 0 otherwise. We note that similar equations have been used by Wolynes and co-workers to study the effect of molecular motors on the actin network [42].

Next, following Wang and Wolynes [43,44], we expand the probability distribution function $\Psi(\mathbf{x}, t)$ in the powers of l up to the quadratic order. This leads to the following effective Fokker-Planck equation

$$\frac{\partial}{\partial t}\Psi(\mathbf{x}, t) = D_{eff}\sum_i[\nabla_i^2 - \beta_{eff}\nabla_i(-\nabla_i U_{eff})]\Psi(\mathbf{x}, t). \quad (4)$$

For Type one enzymes, we have

$$D_{eff} = D + \frac{1}{2}k_1 l^2,$$
$$T_{eff} = TD_{eff}/D,$$
$$U_{eff} = U(\mathbf{x}). \quad (5)$$

For Type two enzymes, we have

$$D_{eff} = D + \frac{1}{2}k_2 l^2\bar{C}$$
$$T_{eff} = TD_{eff}/D$$
$$U_{eff} = U(\mathbf{x}) + \frac{k_2 l}{2D\beta}\sum_i C_{i,i+1}\left[(x_{i,i+1} - \Delta x_{max}) - \frac{l}{2}\right] \quad (6)$$

where $\bar{C} = (1/N)\sum_i\langle C_{i,i+1}\rangle$, and $\langle\cdot\rangle$ represents ensemble averaging. Equations (5) and (6) are the main results of this Letter, and they provide intuitive interpretations for the role of remodeling enzymes in nucleosome positioning. Type one enzymes elevate the system's temperature without perturbing the underlying energy landscape. They may reinforce the intrinsic positioning signals from internucleosome interactions and the DNA sequence by accelerating the rate for the system to approach equilibrium [30]. On the other hand, type two enzymes give rise to an attractive potential between neighboring nucleosomes in addition to a rescaled temperature, and could alter nucleosome position significantly by overwriting thermodynamic effect [31].

To validate the accuracy of the derived effective equilibrium models, we carried out stochastic simulations of the full kinetic model using the Gillespie algorithm [45] to
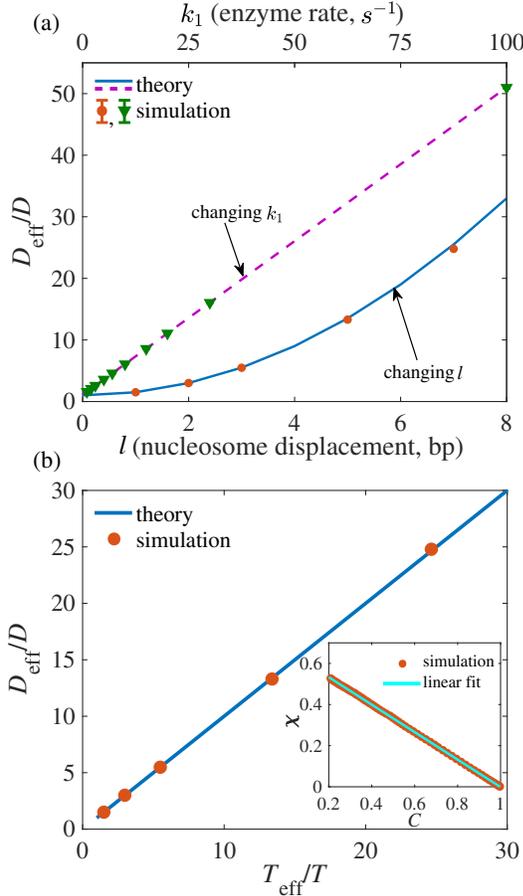
FIG. 2. Comparison between simulated and theoretical values of D_{eff} and T_{eff} for type one enzymes. (a) Dependence of D_{eff} on the enzyme rate k_1 and step size l. (b) T_{eff} determined as the fluctuation-dissipation ratio at $l = 1, 2, 3, 5, 7$ bp and $k_1 = 1$ s^{-1}. Error bars measured as standard deviation of the mean are comparable to the size of the symbols.
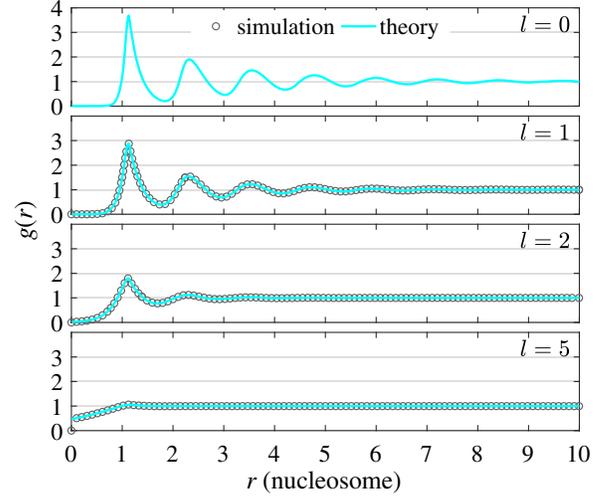

FIG. 3. Comparison between radial distribution functions obtained from nonequilibrium simulations (empty circles) and from theoretical predictions of the effective equilibrium model (cyan lines) for type one enzymes with various step sizes.

obtain "exact" nonequilibrium results. A 58 800 bp long DNA with a total of 400 binding sites was used together with the periodic boundary condition. Only one type of enzymes is included in any given simulation in order to study their effects separately. We used a nucleosome density of 0.8 for simulations with type one enzymes and 0.5 for type two enzymes. These nucleosome densities were chosen to highlight the effect of the enzymes and do not affect our conclusions. More details of these simulations are provided in the Supplemental Material [39].

We first determined the effective diffusion constants for type one enzymes from linear fitting of the mean-squared displacement. As shown in Figs. 2(a) and S1(a), at a fixed rate $k_1 = 1$ s^{-1}, simulated values for D_{eff} (red dots) indeed closely follow the quadratic relationship with l as predicted in Eq. (5) (blue line). We further determined D_{eff} for various enzyme rates k_1 at $l = 1$ bp, and again found excellent agreement between theory (purple line) and numerical simulations (green triangles).

A notable result of the theory is that the fluctuation-dissipation relationship is satisfied with effective parameters. As a test, we determined the effective temperature using the fluctuation-dissipation ratio $\chi(t) = (1/T_{\text{eff}})$ $[C(0) - C(t)]$ [46–49]. We define $\chi(t) = \langle O(t) - O(0) \rangle / h$, $C(t) = \langle O(t + t_o) O'(t_o) \rangle - \langle O(t_o) \rangle \langle O'(t_o) \rangle$, $O(t) = (1/N)$ $\sum_{j=1}^{N} \epsilon_j \exp[i\kappa \cdot x_j(t)]$ and $O'(t) = 2\sum_{j=1}^{N} \epsilon_j \cos[\kappa \cdot x_j(t)]$. ϵ_j are random numbers with values of ± 1 and the wave vector κ is chosen as the value for the first peak of the structure factor [39]. As shown in the inset of Fig. 2(b), a linear relationship is found between $\chi(t)$ and $C(t)$. In the main frame, we plotted T_{eff} for various values of l. The simulated values again agree well with theoretical predictions, and T_{eff} and D_{eff} indeed follow a linear relationship.

To study the usefulness of the effective equilibrium model in predicting steady-state quantities, we computed the radial distribution function [$g(r)$] using nucleosome configurations obtained from simulating type one enzymes at different step sizes. As shown in Figs. 3 and S2(a) as empty circles, consistent with higher effective temperatures, systems with larger step sizes gradually lose their structural ordering, and peaks in $g(r)$ disappear. We further calculated $g(r)$ for effective equilibrium models (cyan lines) using a matrix treatment of the grand partition function proposed by Poland [50], and found that they are in excellent agreement with the ones calculated from kinetic simulations.

Next we study the accuracy of the effective model in describing type two enzymes. As shown in Fig. 4(a), we observed an increase of the diffusion coefficient at larger l due to contributions from ATP driven nucleosome sliding (red dots). The theoretical results (blue dots) were calculated using Eq. (6) with steady-state values for $\bar{C}$ determined from nonequilibrium simulations. Though they
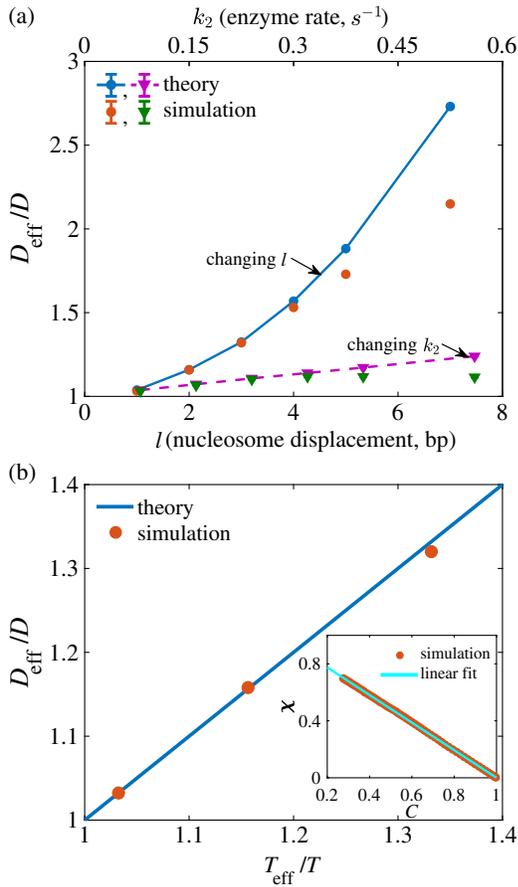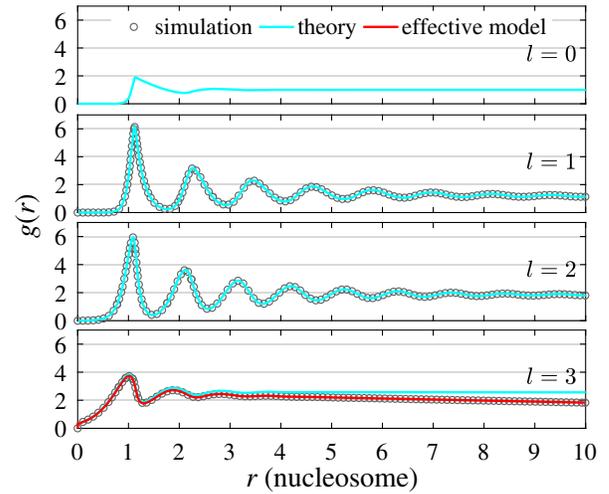
FIG. 5. Comparison between radial distribution functions obtained from nonequilibrium simulations (empty circles) and from theoretical predictions of the effective equilibrium model (cyan lines) for type two enzymes with various step sizes. The red line for $l = 3$ bp was obtained from numerical simulations of the effective equilibrium model.

FIG. 4. Comparison between simulated and theoretical values of D_{eff} and T_{eff} for type two enzymes. (a) Dependence of D_{eff} on the enzyme rate k_2 and step size l. (b) T_{eff} determined as the fluctuation-dissipation ratio at $l = 1, 2, 3$ bp and $k_2 = 0.08$ s^{-1}. Error bars measured as standard deviation of the mean are comparable to the size of the symbols.

agree well at small step sizes, theoretical results begin to deviate significantly from simulation values for $l \geq 5$ bp. Similar behaviors are seen for D_{eff} calculated at different enzyme remodeling rates k_2 (purple and green triangles). Upon close inspection of simulated configurations, we found that the difference between theory and simulation is not due to a failure of the perturbative expansion, but can be attributed to the emergence of overlapping nucleosome configurations and rejection of remodeling steps that result in nucleosomes crossing each other (Fig. S3). It's worth noting that the biological value for l has been estimated to be around 1 bp [51], well within the regime where the theory works. We further followed the same approach as type one enzymes to calculate the effective temperature from the fluctuation dissipation ratio. As shown in Fig. 4(b), T_{eff} again satisfies a linear relationship with D_{eff} as predicted by Eq. (6).

Type two enzymes significantly impact steady-state nucleosome positioning, and $g(r)$ exhibits substantially more peaks even at $l = 1$ bp (empty circles in Fig. 5).

They lead to nucleosome clustering and can significantly increase the timescale needed to reach the steady-state distribution for numerical simulations. We therefore limited our comparison between theory and simulation to small l values. For $l = 1$ and 2 bp, the equilibrium $g(r)$ determined from the effective models (cyan lines) is again in good agreement with steady-state results. For $l = 3$ bp, we carried out stochastic simulations for both the full kinetic model (empty circles) and the effective model (red line) for 1.9×10^8 s to calculate the $g(r)$. These simulations are not long enough to reach steady-state or equilibrium distributions, as the $g(r)$ differs from the true equilibrium result determined from the partition function. However, the simulation results are in excellent agreement with each other, supporting the accuracy of the effective model in predicting time-dependent quantities [see also Fig. S2(b)].

The perturbation theory, therefore, provides a powerful framework to study the role of remodeling enzymes in nucleosome positioning. It further suggests a straightforward strategy to incorporate the impact of remodeling enzymes into existing computational approaches [52–56] for improved prediction of nucleosome positioning *in silico*. In particular, the equilibrium framework adopted in many of these approaches can still be used in the presence of enzymes but with rescaled temperatures and interactions, the values of which can be determined from kinetic parameters of enzymes.

It is important to note that the theory presented here is general and can be directly applied to other nucleosome positioning models that include both types of enzymes (Fig. S4), adopt a different energy form for internucleosome

interactions (Fig. S5), or explicitly account for the effect of DNA sequence (Figs. S6 and S7). Finally, we emphasize that ATP powered motors are crucial for many other essential biological processes [44,57–61]. A general theory for these active, nonequilibrium systems does not exist and is actively sought after by numerous researchers [34,35]. The analytical theory presented here can potentially be a powerful tool for studying such systems and provide insights into their steady-state behaviors.

---

[*]binz@mit.edu

[1] R. K. Richmond, D. F. Sargent, T. J. Richmond, K. Luger, and A. W. Mäder, Crystal structure of the nucleosome core particle at 2.8 Å resolution, Nature (London) **389,** 251 (1997).

[2] K. E. van Holde, *Chromatin*, Springer Series in Molecular Biology (Springer, New York, New York, NY, 1989).

[3] L. Bai and A. V. Morozov, Gene regulation by nucleosome positioning, Trends Genet. **26,** 476 (2010).

[4] L. N. Voong, L. Xi, J.-P. Wang, and X. Wang, Genome-wide mapping of the nucleosome landscape by micrococcal nuclease and chemical mapping, Trends Genet. **33,** 495 (2017).

[5] H. Schiessel, J. Widom, R. F. Bruinsma, and W. M. Gelbart, Polymer Reptation and Nucleosome Repositioning, Phys. Rev. Lett. **86,** 4414 (2001).

[6] W. Möbius, R. A. Neher, and U. Gerland, Kinetic Accessibility of Buried DNA Sites in Nucleosomes, Phys. Rev. Lett. **97,** 208102 (2006).

[7] T. Chou, Peeling and Sliding in Nucleosome Repositioning, Phys. Rev. Lett. **99,** 058105 (2007).

[8] C. Jiang and B. F. Pugh, Nucleosome positioning and gene regulation: Advances through genomics, Nat. Rev. Genet. **10,** 161 (2009).

[9] G. S. Freeman, J. P. Lequieu, D. M. Hinckley, J. K. Whitmer, and J. J. de Pablo, DNA Shape Dominates Sequence Affinity in Nucleosome Formation, Phys. Rev. Lett. **113,** 168101 (2014).

[10] T. Parsons and B. Zhang, Critical role of histone tail entropy in nucleosome unwinding, J. Chem. Phys. **150,** 185103 (2019).

[11] J. Widom, A relationship between the helical twist of DNA and the ordered positioning of nucleosomes in all eukaryotic cells, Proc. Natl. Acad. Sci. U.S.A. **89,** 1095 (1992).

[12] T. Schlick, J. Hayes, and S. Grigoryev, Toward convergence of experimental studies and theoretical modeling of the chromatin fiber, J. Biol. Chem. **287,** 5183 (2012).

[13] Z. Tang *et al.*, CTCF-mediated human 3D genome architecture reveals chromatin topology for transcription, Cell **163,** 1611 (2015).

[14] M. Ohno, T. Ando, D. G. Priest, V. Kumar, Y. Yoshida, and Y. Taniguchi, Sub-nucleosomal genome structure reveals distinct nucleosome folding motifs, Cell **176,** 520 (2019).

[15] P. Fransz and H. De Jong, From nucleosome to chromosome: A dynamic organization of genetic information, Plant J. **66,** 4 (2011).

[16] O. Wiese, D. Marenduzzo, and C. A. Brackley, Nucleosome positions alone can be used to predict domains in yeast chromosomes, Proc. Natl. Acad. Sci. U.S.A. **116,** 17307 (2019).

[17] E. Segal and J. Widom, What controls nucleosome positions?, Trends Genet. **25,** 335 (2009).

[18] K. Struhl and E. Segal, Determinants of nucleosome positioning, Nat. Struct. Mol. Biol. **20,** 267 (2013).

[19] A. L. Hughes and O. J. Rando, Mechanisms underlying nucleosome positioning *in vivo*, Annu. Rev. Biophys. **43,** 41 (2014).

[20] M. Radman-Livaja and O. J. Rando, Nucleosome positioning: How is it established, and why does it matter?, Dev. Biol. **339,** 258 (2010).

[21] R. V. Chereji and D. J. Clark, Major determinants of nucleosome positioning, Biophys. J. **114,** 2279 (2018).

[22] J. Widom, Role of DNA sequence in nucleosome stability and dynamics, Q. Rev. Biophys. **34,** 269 (2001).

[23] S. C. Satchwell, H. R. Drew, and A. A. Travers, Sequence periodicities in chicken nucleosome core DNA, J. Mol. Biol. **191,** 659 (1986).

[24] S. C. Schuster, J. Qi, I. Albert, S. J. Zanton, B. F. Pugh, T. N. Mavrich, and L. P. Tomsho, Translational and rotational settings of H2A.Z nucleosomes across the Saccharomyces cerevisiae genome, Nature (London) **446,** 572 (2007).

[25] E. Segal, Y. Fondufe-Mittendorf, L. Chen, A. Thåström, Y. Field, I. K. Moore, J. P. Z. Wang, and J. Widom, A genomic code for nucleosome positioning, Nature (London) **442,** 772 (2006).

[26] E. Segal and J. Widom, Poly(dA:dT) tracts: Major determinants of nucleosome organization, Curr. Opin. Struct. Biol. **19,** 65 (2009).

[27] N. Krietenstein, M. Wal, S. Watanabe, B. Park, C. L. Peterson, B. F. Pugh, and P. Korber, Genomic nucleosome organization reconstituted with pure proteins, Cell **167,** 709 (2016).

[28] G. J. J. Narlikar, R. Sundaramoorthy, and T. Owen-Hughes, Mechanisms and functions of ATP-dependent chromatin-remodeling enzymes, Cell **154,** 490 (2013).

[29] C. R. Clapier, J. Iwasa, B. R. Cairns, and C. L. Peterson, Mechanisms of action and regulation of ATP-dependent chromatin-remodelling complexes, Nat. Rev. Mol. Cell Biol. **18,** 407 (2017).

[30] R. Padinhateeri and J. F. Marko, Nucleosome positioning in a model of active chromatin remodeling enzymes, Proc. Natl. Acad. Sci. U.S.A. **108,** 7799 (2011).

[31] Y. Zhang, Z. Moqtaderi, B. P. Rattner, G. Euskirchen, M. Snyder, J. T. Kadonaga, X. S. Liu, and K. Struhl, Intrinsic histone-DNA interactions are not the major determinant of nucleosome positions *in vivo*, Nat. Struct. Mol. Biol. **16,** 847 (2009).

[32] N. Kaplan, I. K. Moore, Y. Fondufe-Mittendorf, A. J. Gossett, D. Tillo, Y. Field, E. M. LeProust, T. R. Hughes, J. D. Lieb, J. Widom, and E. Segal, The DNA-encoded

nucleosome organization of a eukaryotic genome, Nature (London) **458**, 362 (2009).

[33] P. B. Becker and W. Hörz, ATP-dependent nucleosome remodeling, Annu. Rev. Biochem. **71**, 247 (2002).

[34] F. S. Gnesotto, F. Mura, J. Gladrow, and C. P. Broedersz, Broken detailed balance and non-equilibrium dynamics in living systems: A review, Rep. Prog. Phys. **81**, 066601 (2018).

[35] U. Seifert, Stochastic thermodynamics, fluctuation theorems and molecular machines, Rep. Prog. Phys. **75**, 126001 (2012).

[36] A. M. Florescu, H. Schiessel, and R. Blossey, Kinetic Control of Nucleosome Displacement by ISWI/ACF Chromatin Remodelers, Phys. Rev. Lett. **109**, 118103 (2012).

[37] J. J. Parmar, J. F. Marko, and R. Padinhateeri, Nucleosome positioning and kinetics near transcription-start-site barriers are controlled by interplay between active remodeling and DNA sequence, Nucleic Acids Res. **42**, 128 (2014).

[38] B. Osberg, O. J. Rando, A. M. Tsankov, W. Mobius, and U. Gerland, Toward a unified physical model of nucleosome patterns flanking transcription start sites, Proc. Natl. Acad. Sci. U.S.A. **110**, 5719 (2013).

[39] See Supplemental Material at http://link.aps.org/supplemental/10.1103/PhysRevLett.123.208102 for analytical derivations, simulation details, and applications of the theory to other nucleosome-positioning models.

[40] T. Owen-Hughes, I. Whitehouse, A. Flaus, B. R. Cairns, M. F. White, and J. L. Workman, Nucleosome mobilization catalysed by the yeast SWI/SNF complex, Nature (London) **400**, 784 (1999).

[41] Z. Zhang, C. J. Wippo, M. Wal, E. Ward, P. Korber, and B. F. Pugh, A packing mechanism for nucleosome organization reconstituted across a eukaryotic genome, Science **332**, 977 (2011).

[42] T. Shen and P. G. Wolynes, Nonequilibrium statistical mechanical models for cytoskeletal assembly: Towards understanding tensegrity in cells, Phys. Rev. E **72**, 041927 (2005).

[43] S. Wang and P. G. Wolynes, Communication: Effective temperature and glassy dynamics of active matter, J. Chem. Phys. **135**, 051101 (2011).

[44] S. Wang and P. G. Wolynes, Tensegrity and motor-driven effective interactions in a model cytoskeleton, J. Chem. Phys. **136**, 145102 (2012).

[45] D. T. Gillespie, Exact stochastic simulation of coupled chemical reactions, J. Phys. Chem. **81**, 2340 (1977).

[46] J. L. Barrat and L. Berthier, Fluctuation-dissipation relation in a sheared fluid, Phys. Rev. E **63**, 012503 (2001).

[47] L. Berthier and J. L. Barrat, Nonequilibrium dynamics and fluctuation-dissipation relation in a sheared fluid, J. Chem. Phys. **116**, 6228 (2002).

[48] L. Berthier and J. L. Barrat, Shearing a Glassy Material: Numerical Tests of Nonequilibrium Mode-Coupling Approaches and Experimental Proposals, Phys. Rev. Lett. **89**, 095702 (2002).

[49] D. Loi, S. Mossa, and L. F. Cugliandolo, Non-conservative forces and effective temperatures in active polymers, Soft Matter **7**, 10193 (2011).

[50] D. Poland, Explicit relations for the radial distribution functions for one-dimensional lattice (arbitrary spacing) fluids and solutions, J. Stat. Phys. **5**, 159 (1972).

[51] W. L. Hwang, B. Bartholomew, S. Deindl, S. K. Hota, P. Prasad, T. R. Blosser, and X. Zhuang, ISWI remodelers slide nucleosomes with coordinated multi-base-pair entry steps and single-base-pair exit steps, Cell **152**, 442 (2013).

[52] V. Miele, C. Vaillant, Y. D'Aubenton-carafa, C. Thermes, and T. Grange, DNA physical properties determine nucleosome occupancy from yeast to fly, Nucleic Acids Res. **36**, 3746 (2008).

[53] A. V. Morozov, K. Fortney, D. A. Gaykalova, V. M. Studitsky, J. Widom, and E. D. Siggia, Using DNA mechanics to predict *in vitro* nucleosome positions and formation energies, Nucleic Acids Res. **37**, 4707 (2009).

[54] T. van der Heijden, J. J. F. A. van Vugt, C. Logie, and J. van Noort, Sequence-based prediction of single nucleosome positioning and genome-wide nucleosome occupancy, Proc. Natl. Acad. Sci. U.S.A. **109**, E2514 (2012).

[55] S. Lubliner and E. Segal, Modeling interactions between adjacent nucleosomes improves genome-wide predictions of nucleosome occupancy, Bioinformatics **25**, i348 (2009).

[56] V. B. Teif, Nucleosome positioning: Resources and tools online, Brief. Bioinform. **17**, 745 (2016).

[57] F. C. Mackintosh and A. J. Levine, Nonequilibrium Mechanics and Dynamics of Motor-Activated Gels, Phys. Rev. Lett. **100**, 018104 (2008).

[58] B. Zhang and P. G. Wolynes, Topology, structures, and energy landscapes of human chromosomes, Proc. Natl. Acad. Sci. U.S.A. **112**, 6062 (2015).

[59] B. Zhang and P. G. Wolynes, Genomic energy landscapes, Biophys. J. **112**, 427 (2017).

[60] Y. Qi and B. Zhang, Predicting three-dimensional genome organization with chromatin states, PLoS Comput. Biol. **15**, e1007024 (2019).

[61] W. J. Xie and B. Zhang, Learning the formation mechanism of domain-level chromatin states with epigenomics data, Biophys. J. **116**, 2047 (2019).